Mon. Not. R. astr. Soc. (1991) **248,** 370–376

White-dwarf rotational equilibria in magnetic cataclysmic variable stars

Brian Warner[1,2] and Dayal T. Wickramasinghe[2]
[1] *Department of Astronomy, University of Cape Town, Rondebosch, South Africa*
[2] *Department of Mathematics, Australian National University, Canberra, Australia*

Accepted 1990 June 13. Received 1990 May 10; in original form 1989 June 12

SUMMARY

The magnetic cataclysmic variable stars (polars, intermediate polars and DQ Her stars) are grouped about three lines in the orbital period–spin period diagram. This segregation is shown to be the consequence of competition between braking and accretion torques when combined with the effects of cyclical variations in rate of mass transfer.

1 INTRODUCTION

The cataclysmic variable stars (CVs), comprising novae, dwarf novae and related stars, consist of close binaries in which Roche-lobe overflow from the secondary star transfers matter to the white-dwarf primary. The path that the transferring gas takes depends strongly on the magnetic field of the white dwarf. For surface fields $B \sim 10^7$ G, the magnetic couple between the stars can lock the white dwarf into synchronous rotation with the binary orbit and gas flows from secondary to primary along the field lines. For low surface fields, the flow is via a stream and an accretion disc that forms around the white dwarf. For intermediate-strength fields, the rotating magnetosphere of the white dwarf is able to disrupt the disc out to a radius which depends on the rate of mass flow through the disc and the spin period of the white dwarf. Sufficiently strong fields are able to prevent the initial formation of the accretion disc, producing discless, asynchronous systems.

The spin period of the white dwarf is determined by competition between the accretion torque produced by the orbital angular momentum of the accreting material, and the braking torques generated through interaction of the primary's magnetic field with the secondary star, the slowly rotating outer parts of the accretion disc, and stellar winds from the secondary and disc (Ghosh & Lamb 1979; Hameury, King & Lasota 1986). For strong enough braking torques, the primary synchronizes with the orbital rotation, i.e. $P_{\rm spin} = P_{\rm orb}$. For lower fields, the primary is spun up to a value near to the rotation period at the inner edge of the accretion disc. This equilibrium spin period is thus determined by the radius of the magnetosphere, R_μ, which is a function of the magnetic moment $\mu\ (=BR_1^3)$ of the primary and the rate of mass transfer $\dot{M}$.

There is observational evidence that in many cataclysmic variables $\dot{M}$ varies by orders of magnitude on time-scales of 10–10^3 yr (Warner 1987). Such time-scales are short compared to the time-scales ($\sim 10^5$ yr) required to spin the primary into equilibrium with the prevailing $\dot{M}$. In such circumstances it might be thought that $P_{\rm spin}$ would be determined simply by some weighted mean $\langle \dot{M} \rangle$, but we show here that for an important group of magnetic cataclysmic variables, the equilibrium value of $P_{\rm spin}$ is governed by cycling between disced and discless mass transfer, and that many of the observed systems indirectly establish the reality of such cycling by obeying the predicted $P_{\rm spin}$–$P_{\rm orb}$ relationship for this process.

2 OBSERVATIONS

The high-field systems, which show highly polarized optical emission and strong keV X-ray emission, are usually known as polars, or AM Her stars after the prototype (Liebert & Stockman 1985). Seventeen are known, in the range $1.3 < P_{\rm orb} < 4$ hr, but with the well-known orbital period gap between $2.1 \lesssim P_{\rm orb} \lesssim 2.9$ hr, in which there is only one magnetic cataclysmic variable (MCV) and only one or two non-magnetic systems. Spectropolarimetry of the polars shows that, in general, they have $2\times10^7 < B < 5\times10^7$ G, or $6\times10^{33} < \mu < 10^{34}$ G cm^3. As $P_{\rm spin} = P_{\rm orb}$ for these systems, we do not list their detailed properties. However, we draw attention to V2051 Oph, for which there is evidence for synchronized spin but no published observations of polarization or X-ray emission. M. S. Cropper (private communication) has observational evidence for orbitally modulated infrared linear polarization in this star, which, if verified by additional observations, will confirm the interpretation by Warner & O'Donoghue (1987) that this is a low-field polar. For $B \lesssim 5\times10^6$ G, no hard X-ray emission is expected and the cyclotron polarization appears principally in the infrared. Such stars are therefore difficult to recognize as polars and may be relatively common.

The non-synchronous systems can be divided into two distinct groups: those showing strong keV X-ray emission and $P_{\rm spin} > 5$ min, and those with no hard X-ray emission and $P_{\rm spin} < 1\frac{1}{2}$ min. These are sometimes collectively called intermediate polars or DQ Herculis stars, but as DQ Her is certainly not typical of the class as a whole, we will employ

Table 1. Observed properties of intermediate polars and DQ Her stars.

Star	P_{orb} (h)	P_{spin}(s)	$\dot{P}_{spin}$ (s.s^{-1})	References
GK Per	47.9	351.34		1
1H0534-581	6.5	7560		2
E1013-477	6.4	4266		3
V426 Oph	6.0	3600*		1
1H0542-407	5.72	1911		2
TV Col	5.49	1911		1,4
FO Aqr	4.85	1254.45	8.0 × 10^{-11}	1,5
1H0551-819	3.9:	937		6
AO Psc	3.59	805.4	-6.6 × 10^{-11}	1,7
V1223 Sgr	3.37	745.43	2.5 × 10^{-11}	1,8
BG CMi	3.24	913.48		1
EX Hya	1.63	4021.61	-9.0 × 10^{-11}	1,9,
SW UMa	1.35	954		10
AE Aqr	9.88	33.08		11
V553 Her	4.99	63.63		12
DQ Her	4.65	71.07	-8.1 × 10^{-13}	7

References: 1. Norton & Watson (1988); 2. Buckley (1988); 3. Mukai & Corbet (1987); 4. Barrett *et al.* (1988); 5, Shafter & Macry (1987); 6. Buckley (private communication); 7. Lamb & Patterson (1985); 8. Pakull & Beuermann (1987); 9. Gilliland (1982); 10. Shafter, Szkody & Thorstensen (1986); 11. Patterson *et al.* (1980); 12. Patterson (1979).
*Other, shorter periods are also compatible with the X-ray observations (Norton & Watson 1988).

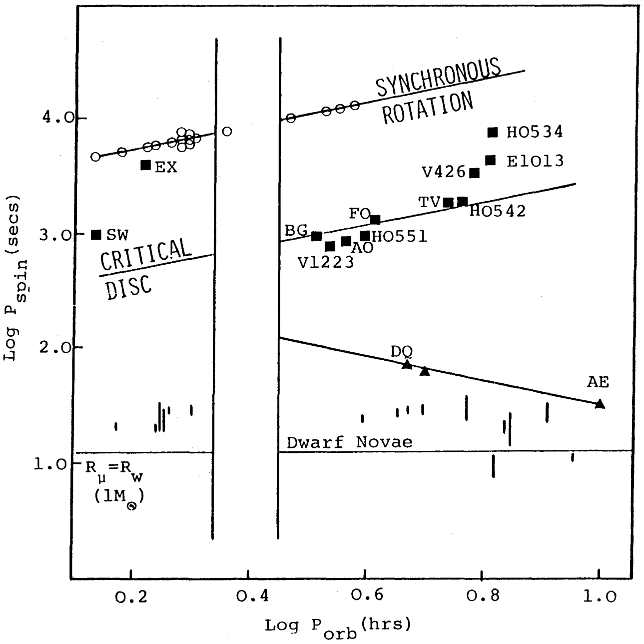

Figure 1. Relationship between spin period P_{spin}, and orbital period, P_{orb}, for polars (synchronous rotation), intermediate polars (critical disc), DQ Herculis stars and Dwarf Novae (short vertical bars).

the distinction now commonly made that the former group are intemediate polars (IPs) and the latter DQ Her stars (Warner 1985). Among the IPs, only BG CMi has so far revealed its magnetic nature through infrared circular polarization (West, Berriman & Schmidt 1987); the interpretation of this is ambiguous – BG CMi could have a μ near the low end of the polar range, or could be a lower-field system. The same uncertainty applies to the group as a whole. However, the DQ Her stars appear almost certainly to be low-field systems, with $\mu \leq 10^{33}$ G cm^3.

Table 1 summarizes the relevant observational properties of the IPs and DQ Her stars.

As was already pointed out by Barrett, O'Donoghue & Warner (1988) (with fewer stars available), in the log P_{spin} versus log P_{orb} diagram (Fig. 1), the IPs above the orbital period gap follow a distinct relationship with relatively little scatter. As the equilibrium value of P_{spin} is determined by μ and $\dot{M}$, at first sight this relationship would appear to imply a connection between μ, $\dot{M}$ and P_{orb}. However, we find that consideration of the effects on P_{spin} of cyclical variations in $\dot{M}$ reveals a less restrictive picture.

3 MASS TRANSFER

Estimates of mass-transfer rates (Warner 1987; Patterson 1984) in CVs, although differing in absolute amounts, agree in showing a large range of $\dot{M}$ at each value of P_{orb}. Above the period gap, the observed range is approximately 10^{16}–2.10^{18} gms s^{-1}, apparently decreasing for $P \gtrsim 6$ hr, and 10^{15}–10^{17} below the gap. As originally pointed out by Verbunt (1984), the lower observed values cannot be characteristic of the secular mean rates of mass transfer $\langle \dot{M} \rangle$: for such low $\dot{M}$, the secondary stars are not driven out of thermal equilibrium and no period gap would occur. The conclusion is that large downward excursions of $\dot{M}$ are superimposed on a $\langle \dot{M} \rangle$ near the upper limit of the observed range.

Many stars with P_{orb} near the period gap, including polars and IPs, are observed to descend into states of low $\dot{M}$ on time-scales ~10 yr (Warner 1985). Other stars (e.g. U Gem) have been observed for many decades without significant change in average $\dot{M}$. For such stars, the variations in $\dot{M}$ must occur on time-scales >100 yr. A possible explanation for a ~10^3-yr time-scale is embodied in the nova hibernation model (Shara *et al.* 1986), in which all CVs cycle through nova, nova-like and dwarf nova stages, their outburst characteristics being determined by the current value of $\dot{M}$. A hundred years or so after a nova explosion $\dot{M}$ falls to a low value (at least for $P_{orb} \lesssim 6$ hr). For longer orbital periods, the range of $\dot{M}$ is predicted to be less extreme and gradually builds up again over ~10^3 yr until the next nova explosion.

Although a CV may currently have a low $\dot{M}$, it is clear from the above that its evolutionary rate, and in particular the value of P_{spin}, will be largely determined by $\langle \dot{M} \rangle$ which lies near the upper value of observed $\dot{M}$, i.e. t(evol) ~ 10^8 yr.

Theoretical investigations (Hameury 1988) of $\dot{M}$ in CVs, based on angular momentum losses through magnetic braking, give values in moderate agreement with the highest observed $\dot{M}$. The observational picture is probably confused by the effects of temporarily enhanced $\dot{M}$ following nova outburst, which may explain why the maximum observed $\dot{M}$ is ~2×10^{18} gm s^{-1}, independent of P_{orb}. A simplified treatment (Hameury *et al.* 1986) of magnetic braking gives $\dot{M} \propto P_{orb}^{5/3}$, but the detailed computation (Hameury *et al.* 1988) of $\dot{M}$ for evolution of a system with initial secondary mass $M_2 = 0.7\ M_\odot$, using the Mestel & Spruit (1987) model of magnetic braking, gives $\dot{M} \propto P_{orb}^{-5/2}$.

Mass transfer in MCVs can take place in two ways: if μ is large enough to dominate gas motions for a substantial fraction of the interstar separation, then the stream of gas from the secondary is broken up by the rotating magnetosphere and the mass transfer is discless. On the other hand, if an accretion disc forms, the mass-transfer stream impacts on the disc to produce a 'bright spot', as in non-magnetic systems, and accretion on to the white dwarf takes place through the magnetospheric zone which disrupts the inner regions of the disc.

Whether individual MCVs have discs or not has been a matter of contention. However, the spectroscopic observations by Penning (1985) and by Buckley (1988), as interpreted by Buckley (1988), argue strongly for the presence of discs – as does the evidence for bright spots. In a discless system most or all of the transferring gas is, at some stage, whirled around with the angular velocity of the white dwarf. This would be expected to lead to large radial velocity variations of the emission lines, modulated with period $P_{\rm spin}$. A search for such modulations by Penning and Buckley in the IPs V1223 Sgr, BG CMi, A0 Psc, F0 Aqr, 1H0542−407 and 1H0534−581 detected the expected modulation periods but with amplitudes much smaller (50–100 km s^{-1}) than predicted by the discless transfer model. Buckley has shown that the observations can be satisfactorily explained by line emission for material corotating with the white dwarf, at the inner edge of an accretion disc.

4 THEORY

The current spin period of a white dwarf in an MCV is determined by μ, the past history of $\dot{M}$ variations, and the nature of the accretion flow. There are four basic distance scales that must be considered when discussing the accretion flow. The Roche-lobe radius, $R_{\rm L}$, of the white dwarf plays a critical role as it determines the distance over which mass and angular momentum are transferred. $R_{\rm L}$ can be estimated from

$$R_{\rm L}=6.9\times10^7\,P(s)_{\rm orb}^{2/3}\,M_1^{1/3}\ {\rm cm}, \tag{1}$$

where M_1 is the mass of the primary in units of solar mass, $M_\odot$. The distance scale on which the magnetic field can significantly influence the flow is given by the Alfven radius R_μ, which is defined as the radius at which the ram pressure of the accretion flow (ρv^2) balances the magnetic pressure ($B^2/8\pi$). R_μ is given by (Hameury *et al.* 1986)

$$R_\mu=2.7\times10^{10}\,\mu_{33}^{4/7}\,\dot{M}_{16}^{-2/7}\,M_1^{-1/7}\,\phi\,{\rm cm}, \tag{2}$$

where $\dot{M}_{16}$ is the rate of accretion in units of 10^{16} gm s^{-1}, μ_{33} (10^{33} G cm^3) is the magnetic moment of the white dwarf and ϕ (≤ 1) is a factor which allows for the deviation of the accretion flow from spherically symmetric infall. For a disc $\phi=0.5$, while for discless accretion ϕ is believed to be close to 0.4.

The third distance scale, $R_{\rm c}$, is the corotation radius defined as the distance from the primary at which its angular velocity equals the Keplerian angular velocity in the disc. $R_{\rm c}$ is given by

$$R_{\rm c}=1.5\times10^8\,P({\rm s})_{\rm spin}^{2/3}\,M_1^{1/3}\ {\rm cm}. \tag{3}$$

Finally, there is a fourth distance scale, R_0, which is defined as the critical radial distance from the primary into which a free-falling accretion stream must penetrate in order that an accretion disc may form. From Lubow & Shu (1975) we find that

$$R_0\simeq0.20\,R_{\rm L}\simeq1.4\times10^7\,P({\rm s})_{\rm orb}^{2/3}\,M_1^{1/3}\ {\rm cm} \tag{4}$$

The above distance scales can be used to determine two important spin periods. First, for disc accretion there is an equilibrium spin period $P_{\rm eq}$(disced) at which the material can accrete on to the white dwarf with zero net torque. This is found by setting $R_\mu=\omega_{\rm s}^{3/2}R_{\rm c}$, where $\omega_{\rm s}$ (≤ 1) is the 'fastness parameter' (Ghosh & Lamb 1979) (and is defined by this equation). We find that

$$P_{\rm eq}({\rm disced})=2440\left(\frac{\mu_{34}}{\sqrt{\dot{M}_{18}}}\right)^{6/7}M_1^{-5/7}\left(\frac{0.35}{\omega_{\rm s}}\right)\left(\frac{\phi}{0.5}\right)^{3/2}\ {\rm s}. \tag{5}$$

Theoretical consideration of the magnetic interaction of the accretion disc with the white dwarf yields $\omega_{\rm s}\simeq0.35$ for zero torque (Ghosh & Lamb 1979). However, this value depends on what is assumed for the pitch angle of the field in its interaction with the disc and it is consequently uncertain.

Secondly, there is an equilibrium spin period $P_{\rm s}$(crit) corresponding to the critical condition that must be satisfied for the formation of a disc, $R_0=\omega_2^{3/2}R_{\rm c}$, which gives

$$P_{\rm s}({\rm crit})=1195\left(\frac{P_{\rm orb}}{4\ {\rm hr}}\right)\left(\frac{0.35}{\omega_{\rm s}}\right)\ {\rm s}. \tag{6}$$

As we described earlier, the accretion rate $\dot{M}$ in the MCVs is expected to exhibit variations on time-scales $\sim10^2$–10^3 yr, as well as a secular change over a much longer ($\sim10^8$ yr) time-scale. As $\dot{M}$ varies from some minimum value $\dot{M}$(min) to a maximum value $\dot{M}$(max), the accretion characteristics of a given system will change. There are four distinct circumstances (see Table 2 for summary).

4.1 Case (a)

At very high magnetic moments $R_\mu>R_{\rm L}$ for all $\dot{M}$, i.e. $\dot{M}({\rm min})\leq\dot{M}\leq\dot{M}({\rm max})$, and a disc cannot form. From equations (1) and (2) the relevant condition is

$$\frac{\mu_{34}}{\sqrt{\dot{M}_{18}({\rm max})}}>7\left(\frac{P_{\rm orb}}{4\ {\rm hr}}\right)^{7/6}M_1^{5/6}\left(\frac{0.5}{\phi}\right)^{7/4}. \tag{7}$$

The white-dwarf spin is braked by magnetic interaction with the intrinsic magnetic field (B_2) of the secondary star, and/or

Table 2.

Case (a)	$\dot{M}$(max)	$R_\mu>R_{\rm L}$	Disc Never Forms (synchronises easily)	
	$\dot{M}$(min)	$R_\mu>R_{\rm L}$		
Case (b)	$\dot{M}$(max)	$R_0<R_\mu<R_{\rm L}$	Disc Never Forms (synchronises)	AM Hers
	$\dot{M}$(min)	$R_\mu>R_{\rm L}$	Disc Never Forms (synchronises)	
Case (c)	$\dot{M}$(max)	$R_\mu<R_0$	Disc Forms	Intermediate Polars
	$\dot{M}$(min)	$R_\mu>0.7R_{\rm L}$	Disc Disrupts	
Case (d)	$\dot{M}$(max)	$R_\mu<R_0$	Permanent Disc Evolution	DQ Hers
	$\dot{M}$(min)	$R_\mu<0.7R_{\rm L}$		

by fields induced in the secondary. In both cases the magnetic torque can be written (Hameury, King & Lasota 1989b) as

$$G_{\mathrm{mag}} = \frac{\mu\mu'}{a^3},$$

where μ' is the magnetic moment (intrinsic or induced) of the secondary. Writing the moment of inertia of the white dwarf as $M_{\mathrm{w}} R_{\mathrm{w}}^2 r_{\mathrm{g}}^2$, where r_{g} is the radius of gyration ($r_{\mathrm{g}}^2 \simeq 0.20$), the synchronization time-scale is

$$t_{\mathrm{syn}} = \frac{M_{\mathrm{w}} R_{\mathrm{w}}^2 r_{\mathrm{g}}^2}{G_{\mathrm{mag}}} \cdot \frac{2\pi}{P_{\mathrm{spin}}}. \tag{8}$$

Setting $M_{\mathrm{w}} = 0.6\ M_{\odot}$ and $R_{\mathrm{w}} = 10^9$ cm we obtain

$$t_{\mathrm{syn}} = 3.5 \times 10^5 \left(\frac{10^3\ \mathrm{s}}{P_{\mathrm{spin}}}\right) \left(\frac{P_{\mathrm{orb}}}{4\ \mathrm{hr}}\right)^2 (\mu_{34}\mu'_{34})^{-1}\ \mathrm{yr}. \tag{9}$$

The accretion torque, which counters magnetic braking, is

$$G_{\mathrm{acc}} = \dot{M} R_{\ell}^2 \Omega,$$

where R_{ℓ} is the 'lever arm' of the accreting gas and Ω is the angular velocity of the arm. For discless accretion, if all of the matter leaving the secondary at the inner Lagrangian point eventually arrives at the primary, we can set $R_{\ell} = R_{\mathrm{L}}$ and $\Omega = 2\pi/P_{\mathrm{orb}}$. The spin-up time-scale is then

$$t_{\mathrm{acc}} = \frac{M_{\mathrm{w}} R_{\mathrm{w}}^2 r_{\mathrm{g}}^2}{G_{\mathrm{acc}}} \cdot \frac{2\pi}{P_{\mathrm{spin}}} \tag{10}$$

$$= 9.5 \times 10^5 \left(\frac{10^3\ \mathrm{s}}{P_{\mathrm{spin}}}\right) \left(\frac{4\ \mathrm{hr}}{P_{\mathrm{orb}}}\right)^{1/3} \dot{M}_{17}^{-1}\ \mathrm{yr}. \tag{11}$$

The ratio $t_{\mathrm{syn}}/t_{\mathrm{acc}}$ depends critically on what is assumed for μ and μ'. If the secondary's magnetic field is of internal dynamo origin, the surface field (Hameury *et al.* 1989a) is $B_2 \simeq 650\, P(\mathrm{hr})_{\mathrm{orb}}^{-1}$ G, yielding $\mu' \simeq 2 \times 10^{34}$ G cm^3 at $P_{\mathrm{orb}} = 4$ hr. The induced magnetic moment ($\propto \mu$) may be more important at high μ, but there are large uncertainties in estimating its magnitude. Taking the intrinsic magnetic moment of the secondary as a lower limit to μ' in equation (9), we find that $t_{\mathrm{syn}}/t_{\mathrm{acc}} \sim 0.3$ for $\dot{M}_{17} = 10$ [for case (a) conditions], so the white dwarf is expected to achieve synchronism on a time-scale that is short compared to the secular evolution time-scale.

There are only four polars for which masses and magnetic fields have been sufficiently well determined to enable μ to be estimated, namely MR Ser ($M_1 = 0.66\ M_{\odot}$, $B = 25$ MG), ST LMi ($M_1 = 0.38$, $B = 19$), EXO 033319 − 2554.2 ($M_1 = 0.94$, $B = 40$) and AM Her ($M_1 = 0.6$, $B = 15$). For these systems, $\mu_{34} = 1.4$, 2.6, 0.8 and 0.7, respectively. It is a curious fact that none of these systems lies in the regime of case (a): if $\dot{M}_{18}(\mathrm{max}) > 0.3$, all except ST LMi violate the inequality equation (7).

This circumstance may be related to the suggestion that polars with sufficiently large μ may undergo accelerated evolution due to additional magnetic braking of the binary through the interaction of the magnetic field of the primary with the stellar wind from the secondary. Calculations (Hameury *et al.* 1989a) suggest that with such cooperative magnetic braking (that is, braking by both stars), the mass of the secondary will be depleted at such a high rate that the system will be driven out of contact on a time-scale much shorter than that for lower-field MCVs. Thus our requirement $R_{\mu} > R_{\mathrm{L}}$ may be more appropriate for accelerated evolution than for mere synchronism.

4.2 Case (b)

At somewhat lower magnetic moments there is a regime where $R_0 < R_{\mu} < R_{\mathrm{L}}$ at $\dot{M}(\mathrm{max})$ and $R_{\mu} > R_{\mathrm{L}}$ at $\dot{M}(\mathrm{min})$. From equations (1), (2) and (4) the conditions (with $\phi = 0.5$) become

$$0.4 \left(\frac{P_{\mathrm{orb}}}{4\ \mathrm{hr}}\right)^{7/6} M_1^{5/6} < \frac{\mu_{34}}{\sqrt{\dot{M}_{18}(\mathrm{max})}} < 7 \left(\frac{P_{\mathrm{orb}}}{4\ \mathrm{hr}}\right)^{7/6} M_1^{5/6}.$$

In this regime, as in case (a), the disc never forms. However, as $R_{\mu} < R_{\mathrm{L}}$ for $\dot{M}(\mathrm{max})$, it is not immediately clear if the white-dwarf spin will synchronize with P_{orb} as in case (a). Our previous estimates (equations 9 and 10) indicate that $t_{\mathrm{syn}}/t_{\mathrm{acc}} \sim 1$ in this regime. It is probable, however, that our estimate for t_{syn} is an upper limit – interaction of the rotating magnetosphere with the accretion stream has been neglected and as this penetrates into regions where the magnetic field is much larger than that which interacts with the secondary, a considerable additional braking torque may be exerted, in which case $t_{\mathrm{syn}} \ll t_{\mathrm{acc}}$ in this regime as well. The fact that many of the well-observed polars lie in this regime strongly supports this view.

4.3 Case (c)

For still lower magnetic moments $R_{\mu} < R_0$ at $\dot{M}(\mathrm{max})$ but $R_{\mu} > 0.7\ R_{\mathrm{L}}$ at $\dot{M}(\mathrm{min})$ (we use the fact that measured disc radii all have radii $\sim 0.7\ R_{\mathrm{L}}$), so the system oscillates between disced and discless states. From equations (1), (2) and (4) the conditions for case (c) are satisfied if

$$\frac{\mu_{34}}{\sqrt{\dot{M}_{18}(\mathrm{max})}} < 0.4 \left(\frac{P_{\mathrm{orb}}}{4\ \mathrm{hr}}\right)^{7/6} M_1^{5/6} \tag{13}$$

and

$$\frac{\mu_{34}}{\sqrt{\dot{M}_{16}(\mathrm{min})}} > 0.4 \left(\frac{P_{\mathrm{orb}}}{4\ \mathrm{hr}}\right)^{7/6} M_1^{5/6}. \tag{14}$$

The condition for a disc to form ($R_{\mu} < R_0$) places an upper limit on μ if it is assumed that $\dot{M}_{18}(\mathrm{max}) \sim 1$. The second condition, equation (14), then implies that the variation in $\dot{M}$ must exceed a factor ~ 100, as is indeed observed to be the case for systems with $P_{\mathrm{orb}} \lesssim 6$ hr. Thus we expect MCVs with $\mu_{34} \lesssim 0.4$ to belong to this category and identify them with the intermediate polars. We note that 8 of the 10 known IPs with $3 < P_{\mathrm{orb}} < 7$ hr lie near the critical line for disc formation, defined by $R_0 = \omega_{\mathrm{s}}^{3/2} R_{\mathrm{c}}$ and given by equation (6), in the $\log P_{\mathrm{spin}} - \log P_{\mathrm{orb}}$ diagram (Fig. 1).

Without additional constraints on the temporal behaviour of $\dot{M}$ the alternating disced–discless evolutionary picture does not immediately lead to a narrow sequence near the critical line in Fig. 1. We note two possible scenarios which can explain the observed narrowness of the IP sequence.

In the first picture we postulate that the braking torque between the white dwarf and the secondary is greatly reduced when the accretion disc forms, so that $t_{syn}/t_{acc} \gg 1$ during the phases of disced evolution, reverting to <1 during discless evolution. If, in addition, the variations of $\dot{M}$ are weighted towards $\dot{M}$(max), we expect a relatively narrow sequence in the log P_{spin}–log P_{orb} diagram, with each system driven mostly towards the IP line and rarely towards the polar line. This scenario follows naturally from our discussion of case (b), where we showed that an efficient synchronizing mechanism must be acting during discless evolution in order to explain the presence of the polars in the case (b) regime.

Alternatively, a system may be driven between the disced equilibrium period P_{eq}(disced) (equation 5) and the discless equilibrium period P_{eq}(discless). For the latter, the equilibrium period is given by the condition $R_\mu = R_c$ (i.e. $\omega_s = 1$). If we adopt $\phi = 0.37$ for the discless state, equation (5) yields

$$P_{eq}(\text{discless}) \approx 5\,P_{eq}(\text{disced}). \qquad (15)$$

Although the numerical factor in this equation is uncertain, the standard theory of disced and discless accretion leads to P_{eq}(discless) $> P_{eq}$(disced).

When a disc is established the primary is torqued by gas at the inner edge of the accretion disc; the accreted specific angular momentum is less than in the discless case because any particle that reaches the inner edge of the disc must have lost angular momentum to other particles in the disc. A further source of braking appears as the magnetic field of the primary interacts with the slower-rotating outer parts of the disc. Now $R_\ell = R_\mu$ and the time-scale for spin-up becomes

$$t_{spin} = \frac{M_w R_w^2 r_g^2}{\dot{M} R_\mu^2} \qquad (16)$$

$$\simeq 4.5 \times 10^5\, \mu_{33}^{-8/7}\, \dot{M}_{17}^{-3/7}\ \text{yr}.$$

Whatever the initial spin period, when mass transfer first starts, both discless and disced evolution will drive P_{spin} towards a value near the two possible values of P_{eq}. When this has been achieved – on a time-scale which is short when compared with orbital evolution – competition begins between the effects of disced and discless evolution, and a (non-stationary) mean value is achieved. We expect this value to be close to P_s(crit).

In reality, both mechanisms should operate: those case (c) MCVs which initially spend most of their time in the discless state are rapidly driven into synchronism, while those that are predominantly disced survive as IPs and naturally find an equilibrium spin period near P_{eq}(disced) that is close to P_s(crit), as is indeed observed for the IPs. The chances of finding a system in which the combination of μ and temporal variation of $\dot{M}$ lead to a stable P_{spin}, neither near P_{orb} nor near P_{eq} (disced), are small, with the result that the space between the $P_{spin} = P_{orb}$ line and the $P_{spin} = P_s$(crit) line in Fig. 1 is devoid of stars.

The observed existence of both positive and negative values of $\dot{P}_{spin}$ (Table 1) is supportive evidence for the alternating cycle of spin-up and spin-down.

Hameury *et al.* (1989b) have investigated the effects of $\dot{M}$ variations on time-scales $\sim 10^5$ yr (i.e. comparable to spin-up time-scales). Under such conditions, polars can become desynchronized, leading to interchange between polars and IPs. On the shorter time-scales ($\sim 10^3$ yr) considered here, although for μs at the lower end of the polar range the rotation of polars may become slightly desynchronized near maximum $\dot{M}$, this will generally be a short-lived condition with low probability of discovery.

Finally we note that there are a few IPs near $P_{orb} = 6$ hr which do not follow the critical disc line. We suggest that these are systems which do not experience the variation in $\dot{M}$ (a factor of $\gtrsim 100$) required for case (c). Such systems belong to case (d) (see below), which are characterized by permanent discs.

4.4 Case (d)

The upper limit to the magnetic moment consistent with the formation of a disc at $\dot{M}$(max) ($R_\mu < R_0$) has already been discussed. In the final category we consider systems for which the variation of $\dot{M}$ (or the value of μ) is such that the disc never disrupts (i.e. $R_\mu < 0.7\ R_L$). These conditions can be written (with $\phi = 0.5$) as

$$\frac{\mu_{34}}{\sqrt{\dot{M}_{18}(\text{min})}} < 0.4 \left(\frac{P_{orb}}{4\ \text{hr}}\right)^{7/6} M_1^{5/6} \qquad (17)$$

and

$$\frac{\mu_{34}}{\sqrt{\dot{M}_{16}(\text{min})}} < 0.4 \left(\frac{P_{orb}}{4\ \text{hr}}\right)^{7/6} M_1^{5/6}. \qquad (18)$$

We define $\alpha = \dot{M}(\text{min})/\dot{M}(\text{max})$; then equations (17) and (18) can be written

$$\mu_{34} < 0.4 \left(\frac{P_{orb}}{4\ \text{hr}}\right)^{7/6} M_1^{5/6} \sqrt{\dot{M}_{18}(\text{max})} \quad \text{for} \quad \alpha > 0.01 \qquad (19)$$

$$\mu_{34} < 0.4\sqrt{100\,\alpha} \left(\frac{P_{orb}}{4\ \text{hr}}\right)^{7/6} M_1^{5/6} \sqrt{\dot{M}_{18}(\text{max})} \ \text{for}\ \alpha < 0.01. \qquad (20)$$

These are upper bounds of μ_{34}, depending on the amplitude of the variation of $\dot{M}$ and the absolute value of $\dot{M}_{18}$(max). For small range of $\dot{M}$ the objects will lie anywhere in the log P_{spin}–log P_{orb} diagram (e.g. H0534 and E1013). For large variations in $\dot{M}$ ($\alpha < 1/100$), the continuous disc systems occur only for low values of μ, and the upper bound on μ now depends on the range of $\dot{M}$. We thus have a natural way of accounting for the DQ Her stars as systems which are in disc equilibria appropriate to $\langle \dot{M} \rangle \sim \dot{M}$(max) (where most of the torque occurs), and characterized by large variations of $\dot{M}$. The position of the DQ Her sequence depends sensitively on $\dot{M}$(max) and α. For DQ Her itself, $\dot{M}_{18}$(max) ~ 1 and $P_{spin} = 71$ s. Equation (5) then yields

$$\frac{\mu_{34}}{\sqrt{\dot{M}_{18}(\text{max})}} = 0.016. \qquad (21)$$

Adopting $\dot{M}_{18}$(max) $= 1$, the condition (20) then requires $\alpha = 10^{-5}$. That is, $\dot{M}$ must vary over the range $10^{13} \le \dot{M} \le 10^{18}$ gm s^{-1}. If DQ Her (the remnant of Nova Herculis 1934) follows the behaviour (Shara, Moffat &

Webbink 1985) of the nova remnants Nova Vul 1672 and Nova Sge 1783, it will indeed, over the next century or two, experience a fall in $\dot{M}$ to the very low values required by our scenario (and has done so many times during earlier post-nova episodes).

It is interesting to note that the DQ Her stars lie close to the value of μ below which the magnetic field is expected to be submerged in the photosphere of the white dwarf. This condition, obtained from $R_\mu \geq R_w$, is

$$\frac{\mu_{34}}{\sqrt{\dot{M}_{18}}} \geq 0.0066\ M_1^{-1/3}, \qquad (22)$$

where we have used the approximation $R_w = 7.9 \times 10^8\ M_1^{-1/3}$ cm. As shown in the next section, this relationship may have great relevance to the nature of the rapid oscillations seen in many dwarf novae during outburst.

The observations (Table 1) show that the few known DQ Her stars above the period gap have spin periods that are systematically lower at longer orbital periods, following closely a relationship $P_{spin} \times P_{orb} = \text{constant}$. This can be explained if we adopt the $\dot{M}(P_{orb})$ functional relationship that is given by the Mestel & Spruit (1987) model

$$\dot{M} = 1.3 \times 10^{17} \left(\frac{P_{orb}}{4\ \text{hr}}\right)^{5/2} \text{gm s}^{-1}\ (3 \lesssim P \lesssim 10\ \text{hr}), \qquad (23)$$

but we increase the rate to $\dot{M} = 1.0 \times 10^{18}$ gm s^{-1} at $P_{orb} = 4$ hr to be in better agreement with the observed $\dot{M}$(max) rates. Then from equations (5) and (23) we have

$$P_{spin} = 2440\ \mu_{34}^{6/7} \left(\frac{4\ \text{hr}}{P_{orb}}\right)^{15/14} M_1^{-5/7} \left(\frac{0.35}{\omega_s}\right)\left(\frac{\phi}{0.5}\right)^{3/2}, \qquad (24)$$

which yields a line that passes through the DQ Her stars if $\mu_{34} = 0.016$.

5 DWARF NOVA OSCILLATIONS

In addition to the strictly coherent oscillations seen in the DQ Her stars, rapid oscillations of lower coherence and variable period are seen in dwarf novae during outburst and in some nova-like systems (which can be thought of as dwarf novae in permanent outburst). The observed periods (see table 5.1 of Warner 1988) cover the range 7.5–40 s. Individual stars with their observed ranges of period are plotted in Fig. 1 and it is evident that the DQ Her line forms an upper boundary to the dwarf nova oscillations (DNO). These oscillations are therefore at periods close to the lowest permitted by the condition $R_\mu \geq R_w$. If, as has long been suspected, the DNO are unstable versions of the magnetically controlled DQ Her star spin rates, with magnetic moments even smaller than in the DQ Her stars, so they have been spun up almost to break-up point, then we may expect that their P_{spin} values will be bounded approximately by the condition $R_\mu \geq R_w$, which, from equations (5) and (22), gives

$$P_{spin} \gtrsim 34\ M_1^{-1}. \qquad (25)$$

This equation, which is nothing more than $P_{spin} \geq \omega_s^{-1} \times$ (period of Keplerian orbit at surface of white dwarf) with $\omega_s = 0.35$, is clearly limited in its applicability by uncertainty of the appropriate value of ω_s in such an extreme situation. In fact, the observations seem to be bounded by $P_{spin} \lesssim 12\ M_1^{-1}$ s, i.e. with $\omega_s \simeq 1$.

As equation (25) (or any modified form with appropriate ω_s) is independent of μ and $\dot{M}$, the frequency distribution of the lowest observed periods of the DNO could be closely related to the frequency distribution of masses of the white dwarfs in CVs. Transformation of the histogram of DNO observed minimum periods to a histogram of masses through $P_{spin} = 12\ M_1^{-1}$ s does indeed produce a mass function with a narrow peak near 0.6 $M_\odot$ and a tail to high masses which looks very similar to the mass function for isolated white dwarfs.

6 MCVs BELOW THE GAP

The picture that we have developed suggests that the magnetic moments of IPs above the period gap are in general lower than those of the polars and could have a substantial spread (factor of 3–10) below the polar lower limit (currently set by AM Her with $\mu_{34} \simeq 0.6$). This is an inevitable consequence of our model for the five objects above the period gap in the period range ($3 \lesssim P_{orb} \lesssim 4$ hr) where both polars and intermediate polars are observed. It is likely that this conclusion holds for all objects on the critical disc line up to $P_{orb} \simeq 6$ hr. We cannot exclude the possibility that the two stars (1H0534 and E1013) near $P_{orb} = 6$ hr may have μs in the range of the polars, since they are not in the disced–discless regime in the log P_{spin}–P_{orb} diagram. If so, they will become synchronized when they evolve to shorter orbital periods.

We expect the majority of the IPs to stay close to the critical disc line until they reach the period gap. When accretion ceases all IPs will synchronize on a time-scale $\sim 2 \times 10^6$ yr (equation 9). Below the period gap the braking torque ($\propto 1/a^3$) could be relatively more important in comparison to the accretion torque ($\propto \dot{M}$) since a and $\langle \dot{M} \rangle$ are smaller. Although braking through interaction of the intrinsic field of the secondary will be lower and will probably be negligible compared with that of the induced field, there are large uncertainties in calculations of the latter so it is not clear whether magnetic braking of the primary spin will be more or less effective when systems emerge from the period gap. If we take $\mu' \sim \frac{1}{2}\mu$ as an upper limit to the induced moment, then equations (9) and (10) show that t_{syn}/t_{acc} decreases by a factor of 25 (for $\mu_{34} = 1$) between $P_{orb} = 3$ and 2 hr as $\dot{M}$ decreases by a factor of 10.

Some of the IPs, near the top end of their μ distribution, may remain synchronized after they emerge from the gap. However, the observations do not show any evidence for a systematic decrease in μs below the gap; indeed, AM Her has the smallest μ of the well-observed polars and is above the gap. This suggests that most of the known polars below $P_{orb} \sim 2$ hr must have evolved as polars at least for $P_{orb} \lesssim 5$ hr.

What then is the fate of IPs as they evolve below the period gap? We argue in a subsequent paper (Wickramasinghe, Wu & Ferrario 1990) that the majority of these objects will evolve into systems which are asynchronous but accrete without a disc most of the time. Due to the nature of the accretion process (clumpy rather than smooth), the accretion energy will be emitted mainly at EUV energies ($T \sim 2 \times 10^5$ K). These systems will not distinguish themselves as hard, or soft X-ray emitters and remain undetected in the presently available X-ray surveys.

As pointed out by Hameury *et al.* (1986), the position and $\dot{P}_{spin}<0$ of EX Hya can be understood if it has recently emerged from the period gap and is spinning up towards equilibrium.

7 CONCLUSION

The distinctive grouping of stars in the log P_{spin}–log P_{orb} diagram (Fig. 1) does not imply restricted ranges of magnetic moment μ, or special correlations between P_{spin}, P_{orb} and μ. The distribution of objects in Fig. 1 is readily explained by the interaction of braking torques and accretion torques, with the superposition of the observed or implied variations of $\dot{M}$ on time-scales $>10^2$ yr, acting on a continuum of magnetic moments.

REFERENCES

Barrett, P., O'Donoghue, D. & Warner, B., 1988. *Mon. Not. R. astr. Soc.*, **233**, 759.

Buckley, D. A. H., 1988. *PhD thesis*, Australian National University.

Ghosh, P. & Lamb, F. K., 1979. *Astrophys. J.*, **234**, 296.

Gilliland, R. L., 1982. *Astrophys. J.*, **258**, 576.

Hameury, J. M., King, A. R. & Lasota, J.-P., 1986. *Mon. Not. R. astr. Soc.*, **218**, 695.

Hameury, J. M., King, A. R. & Lasota, J. P., 1989a. *Astrophys. J.*, **344**, 376.

Hameury, J. M., King, A. R. & Lasota, J. P., 1989b. *Mon. Not. R. astr. Soc.*, **237**, 39.

Hameury, J. M., King, A. R., Lasota, J. P. & Ritter, H., 1988. *Mon. Not. R. astr. Soc.*, **231**, 535.

Lamb, D. Q. & Patterson, J., 1985. In: *Cataclysmic Variables & Related Objects*, p. 229, eds Livio, M. & Shaviv, G., Reidel, Dordrecht.

Liebert, J. & Stockman, H. S., 1985. In: *Cataclysmic Variables & Low Mass X-ray Binaries*, p. 151, eds Lamb, D. Q. & Patterson, J., Reidel, Dordrecht.

Lubow, S. H. & Shu, F. H., 1975. *Astrophys. J.*, **198**, 383.

Mestel, L. & Spruit, H. C., 1987. *Mon. Not. R. astr. Soc.*, **226**, 57.

Mukai, K. & Corbet, R. H. D., 1987. *Publs astr. Soc. Pacif.*, **99**, 149.

Norton, A. J. & Watson, M. G., 1988. *Mon. Not. R. astr. Soc.*, **237**, 853.

Pakull, M. & Beuermann, K., 1987. *Astrophys. Space Sci.*, **130**, 641.

Patterson, J., 1979. *Astrophys. J.*, **233**, L13.

Patterson, J., 1984. *Astrophys. J. Suppl.*, **54**, 443.

Patterson, J., Branch, D., Chincarini, G. & Robinson, E. L., 1980. *Astrophys. J.*, **240**, L133.

Penning, W. R., 1985. *Astrophys. J.*, **289**, 300.

Shafter, A. W. & Macry, J. D., 1987. *Mon. Not. R. astr. Soc.*, **228**, 193.

Shafter, A. W., Szkody, P. & Thorstensen, J., 1986. *Astrophys. J.*, **308**, 765.

Shara, M. M., Moffat, A. F. J. & Webbink, R. N., 1985. *Astrophys. J.*, **294**, 271.

Shara, M. M., Livio, M., Moffat, A. F. J. & Orio, M., 1986. *Astrophys. J.*, **311**, 163.

Verbunt, F., 1984. *Mon. Not. R. astr. Soc.*, **209**, 227.

Warner, B., 1985. In: *Cataclysmic Variables & Low Mass X-ray Binaries*, p. 269, eds Lamb, D. Q. & Patterson, J., Reidel, Dordrecht.

Warner, B., 1987. *Mon. Not. R. astr. Soc.*, **227**, 23.

Warner, B., 1988. *High Speed Astronomical Photometry*, Cambridge University Press, Cambridge.

Warner, B. & O'Donoghue, D., 1987. *Mon. Not. R. astr. Soc.*, **224**, 733.

West, S. C., Berriman, G. & Schmidt, G. D., 1987. *Astrophys. J.*, **322**, L35.

Wickramasinghe, D. T., Wu, K. & Ferrario, L., 1990. Preprint.